PHYSICAL REVIEW B **85**, 224505 (2012)

Pure dephasing in flux qubits due to flux noise with spectral density scaling as $1/f^{\alpha}$

S. M. Anton,[1] C. Müller,[2,3] J. S. Birenbaum,[1] S. R. O'Kelley,[1] A. D. Fefferman,[1,*] D. S. Golubev,[4] G. C. Hilton,[5] H.-M. Cho,[5] K. D. Irwin,[5] F. C. Wellstood,[6] Gerd Schön,[4,7] A. Shnirman,[2] and John Clarke[1]

[1]*Department of Physics, University of California, Berkeley, California 94720-7300, USA*
[2]*Institut für Theorie der Kondensierten Materie, Karlsruhe Institute of Technology, D-76128 Karlsruhe, Germany*
[3]*Département de Physique, Université de Sherbrooke, Sherbrooke, Québec, Canada J1K 2R1*
[4]*Institut für Nanotechnologie, Karlsruhe Institute of Technology, D-76021 Karlsruhe, Germany*
[5]*National Institute of Standards and Technology, Boulder, Colorado 80305-3337, USA*
[6]*Joint Quantum Institute, Department of Physics, University of Maryland, College Park, Maryland 20742, USA*
[7]*Institut für Theoretische Festkörperphysik, Karlsruhe Institute of Technology, D-76128 Karlsruhe, Germany*

(Received 28 November 2011; revised manuscript received 16 February 2012; published 5 June 2012)

For many types of superconducting qubits, magnetic flux noise is a source of pure dephasing. Measurements on a representative dc superconducting quantum interference device (SQUID) over a range of temperatures show that $S_\Phi(f) = A^2/(f/1\ \mathrm{Hz})^\alpha$, where S_Φ is the flux noise spectral density, A is of the order of 1 $\mu\Phi_0\ \mathrm{Hz}^{-1/2}$, $0.61 \leqslant \alpha \leqslant 0.95$, and Φ_0 is the flux quantum. For a qubit with an energy level splitting linearly coupled to the applied flux, calculations of the dependence of the pure dephasing time τ_ϕ of Ramsey and echo pulse sequences on α for fixed A show that τ_ϕ decreases rapidly as α is reduced. We find that τ_ϕ is relatively insensitive to the noise bandwidth, $f_1 \leqslant f \leqslant f_2$, for all α provided the ultraviolet cutoff frequency $f_2 > 1/\tau_\phi$. We calculate the ratio $\tau_{\phi,E}/\tau_{\phi,R}$ of the echo (E) and Ramsey (R) sequences and the dependence of the decay function on α and f_2. We investigate the case in which $S_\Phi(f_0)$ is fixed at the "pivot frequency" $f_0 \neq 1$ Hz while α is varied and find that the choice of f_0 can greatly influence the sensitivity of $\tau_{\phi,E}$ and $\tau_{\phi,R}$ to the value of α. Finally, we present calculated values of τ_ϕ in a qubit corresponding to the values of A and α measured in our SQUID.

DOI: 10.1103/PhysRevB.85.224505 PACS number(s): 85.25.Dq, 03.67.Lx, 05.40.Ca

I. INTRODUCTION

The dynamics of superconducting quantum bits (qubits)[1]—broadly classified as charge qubits,[2] flux qubits,[3] and phase qubits[4]—can be characterized by two times: the relaxation time T_1 and the pure dephasing time τ_ϕ.[5] The time T_1 required for a qubit to relax from its first excited state to its ground state is determined by the strength of environmental fluctuations at a frequency corresponding to the energy level splitting ν_{01} of the two states. The decoherence time T_2, over which the phase of superpositions of two eigenstates becomes randomized, has two contributions: $1/T_2 = 1/(2\,T_1) + 1/\tau_\phi$. The pure dephasing time τ_ϕ is limited by fluctuations in ν_{01}, due predominantly to fluctuations in magnetic flux in the case of flux qubits.

Excess low-frequency flux noise was first identified in dc superconducting quantum interference devices (SQUIDs).[6] Measurements at millikelvin temperatures[7–10] reveal a power spectrum $S_\Phi(f)$ scaling as $1/f^\alpha$ (f is frequency), with an amplitude at 1 Hz typically of the order of 1 $\mu\Phi_0\ \mathrm{Hz}^{-1/2}$, that is surprisingly uniform for SQUID washers of widely differing geometries that are fabricated with a variety of materials. Here $\Phi_0 \equiv h/2e$ is the flux quantum.

Flux noise is believed to arise from the random reversal of electron spins at the interface between a superconducting film and an insulator.[11–13] The areal density of independent spins required to account for the observed flux noise is about $5 \times 10^{17}\mathrm{m}^{-2}$, a value that has been corroborated by observations of paramagnetism in SQUIDs[9] and normal metal rings.[14] Recent experiments on anticorrelations of flux noise have confirmed the surface spin model.[15,16] An unambiguous understanding of the mechanism by which the spins produce $1/f$ flux noise, however, has yet to be developed. Recent proposals include spin clusters,[17] spin glasses,[18] fractal spin clusters,[19] and hyperfine interactions;[20] the models in Refs. 18 and 19 suggest that α may differ from unity.

Measurements of τ_φ in flux qubits[15,16,21–23] and phase qubits[24] have been used to infer the magnitude of the flux noise in these devices, under the assumption that the spectral density of the flux noise scaled as $1/f$. In this paper we first present measurements of flux noise spectral densities scaling as $1/f^\alpha$ in which the exponent α deviates markedly from unity. We then show theoretically that such deviations strongly affect τ_φ: The value of τ_φ decreases markedly with decreasing α. Additionally, we examine the influence of α and noise bandwidth on τ_ϕ, the ratio $\tau_{\phi,E}/\tau_{\phi,R}$ obtained in echo (E) and Ramsey (R) pulse sequences, and the functional dependence of the decay function. Finally, we calculate the predicted τ_ϕ for values of A and α obtained in our measurements.

II. EXPERIMENTAL PROCEDURES AND RESULTS

We measured the flux noise spectral densities of Nb-based dc SQUIDs, fabricated using a 50-A/cm^2 Nb/AlO$_x$/Nb trilayer process.[25] Each 2.5 × 2.5-μm^2 junction was shunted with a 2.5-Ω PdAu resistor to eliminate hysteresis on the current-voltage (I-V) characteristic. Up to six SQUIDs, connected in series, were, in turn, connected in series with a compensating resistor $R_c \approx 0.45\Omega$ and the superconducting input coil of a readout SQUID, operated in a flux-locked loop (Fig. 1). To measure the noise in a given SQUID, we applied a current I_b sufficient to produce a voltage V of, typically, 5 μV across it. The resulting static current around the circuit was canceled by an appropriate current I_r in R_c to ensure that the remaining SQUIDs remained in the zero-voltage state. In

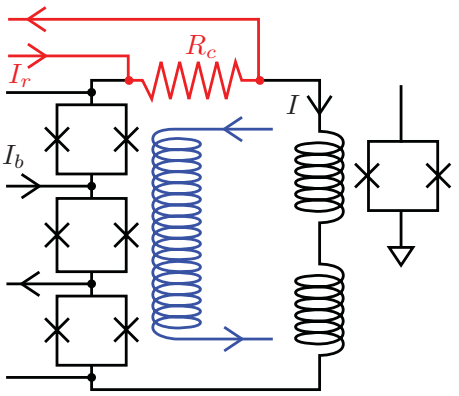

FIG. 1. (Color online) Circuit schematic of measurement system for three measured SQUIDs. Measurement of the middle SQUID is shown (see text). A single coil applies flux to all SQUIDs.

addition, a choke inductor was used to decouple oscillations at the Josephson frequency between the measured and readout SQUIDs. Since R_c was much less than the dynamic resistance of any given SQUID, the SQUID was effectively voltage biased. Fluctuations in the critical current of the measured SQUID induced a current noise I with spectral density $S_I(f)$ in the input coil of the readout SQUID. We inferred the flux noise from $S_\Phi(f) = S_I(f)/[(\partial I/\partial\Phi)_V]^2$, where Φ is the flux applied via an external coil to the measured SQUID and $(\partial I/\partial\Phi)_V$ was determined separately. We also measured the critical current noise of the junctions[6] in each SQUID biased at $n\Phi_0$ (n is an integer) so $(\partial I/\partial\Phi)_V = 0$. This noise was negligible compared with the current noise produced by the flux noise for large values of $(\partial I/\partial\Phi)_V$. The experiment was mounted in a lead-coated copper box surrounded by a cylindrical lead shield inside a cryoperm shield and cooled with a dilution refrigerator. All leads were heavily filtered.

Figure 2 shows power spectra of a single SQUID at three different temperatures. The inner and outer dimensions of the washer were 50 and 90 μm, respectively. At higher frequencies, the spectra begin to flatten out due to white current noise from the SQUID shunt resistors, which dominates that from R_c. The spectra were fitted to the form

$$S(f) = A^2/(f/1\ \text{Hz})^\alpha + C^2 \tag{1}$$

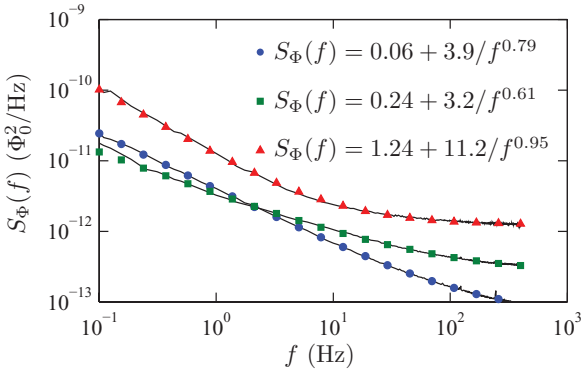

FIG. 2. (Color online) Measured and fitted flux noise spectra. Measured spectra at 0.2, 1.3, and 4.5 K are continuous curves; symbols are fits to Eq. (1). Quoted values in the fits are in units of $(\mu\Phi_0)^2$/Hz.

with parameters A and C for the amplitude of the "$1/f$" flux noise and white noise, respectively. We found that the exponent α of the $1/f^\alpha$ noise can be far from unity, varying from 0.61 to 0.95. We remark that these values are representative of measurements on about 20 SQUIDs. Since the junctions in flux qubits are not resistively shunted, we shall focus on dephasing from the term $A^2/(f/1\ \text{Hz})^\alpha$.

III. THEORETICAL RESULTS

A. Model

Since α can evidently be much less than unity, it is natural to ask what impact this has on the pure dephasing of flux qubits. Low-frequency flux noise modulates the energy splitting of the ground and first excited states of a flux qubit, $h\nu_{01} = [\Delta^2 + \epsilon^2(\Phi)]^{1/2}$, via the bias energy $\epsilon(\Phi)$. The bias energy is the energy difference between the two states with persistent currents $\pm I_q$ when there is no tunneling between them ($\Delta = 0$).[26] Here $\epsilon = 2I_q(\Phi - \Phi_0/2)$ or, equivalently, $I_q \equiv \frac{1}{2}(\partial\epsilon/\partial\Phi)$.

We define the sensitivity of the splitting to a change in Φ in terms of the longitudinal sensitivity of the qubit to flux noise,

$$D_\Phi \equiv \partial\nu_{01}/\partial\Phi = (1/h)(\partial\epsilon/\partial\Phi)\epsilon/(\Delta^2 + \epsilon^2)^{1/2}. \tag{2}$$

To first order, there is no dephasing from flux noise at the degeneracy point, $\Phi = \Phi_0/2$, where ϵ vanishes. In this paper, however, we consider the limit $\epsilon/\Delta \gg 1$, far from the degeneracy point, at which $\partial\nu_{01}/\partial\Phi = (1/h)\partial\epsilon/\partial\Phi = 2I_q/h$. We assume that, in this limit, $1/\tau_\phi \gg 1/2T_1$ so the measured dephasing time arises only from pure dephasing. We adopt the value $D_\Phi = 10^{12}$ Hz/Φ_0, corresponding to the typical value[21,22] $I_q \approx 0.3\ \mu$A. Furthermore, based on the empirical observation that $S_\Phi(1\ \text{Hz})$ is relatively constant among a wide variety of SQUIDs, we assume that $A = 1\mu\Phi_0\ \text{Hz}^{-1/2}$ regardless of the value of α. We consider noise fixed at a frequency other than 1 Hz in Sec. III F.

The modulation of ν_{01} by flux noise leads to an accumulation of phase error and, thus, to dephasing. The rate at which the dephasing occurs varies between different types of pulse sequences. For example, in a Ramsey sequence[27] the qubit is excited by a microwave $\pi/2$ pulse from the ground state into a superposition of ground and excited states. After a time t another $\pi/2$ pulse is applied and the qubit state is measured. The results of many measurements with fixed t are averaged and t is varied from $t \ll \tau_\phi$ to $t \gg \tau_\phi$ to obtain the decay function $g(t)$. Here, we define the dephasing time as $g(\tau_\phi) \equiv 1/e$. To eliminate dephasing due to flux fluctuations between pulse sequences, one implements an echo sequence in which a π pulse is inserted midway between the two $\pi/2$ pulses.[28] In general, the echo sequence yields a dephasing time greater than that of the Ramsey: $\tau_{\phi,E} > \tau_{\phi,R}$.

The sensitivity of the Ramsey and echo sequences to noise are described by the weighting function $W(f,t)$ given by[4,29]

$$W_R(f,t) = \frac{\sin^2(\pi f t)}{(\pi f t)^2}, \qquad W_E(f,t) = \frac{\sin^4(\pi f t/2)}{(\pi f t/2)^2}. \tag{3}$$

For the Ramsey sequence with $f \ll 1/t$, we see that $W_R \approx 1$, whereas for $f \gg 1/t$, W_R falls as $1/f^2$. Consequently, we expect the dominant contributions to the Ramsey dephasing

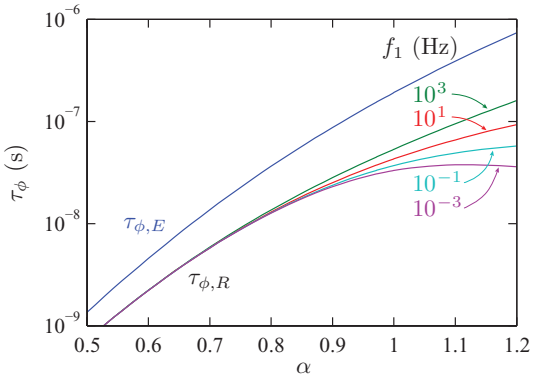

FIG. 3. (Color online) Computed values of $\tau_{\phi,R}$ and $\tau_{\phi,E}$ vs. α for $f_1 = 10^{-3}$, 0.1, 10, and 10^3 Hz and $f_2 \to \infty$.

time to arise from noise at frequencies $f \lesssim 1/\tau_{\phi,R}$. In contrast, for the echo sequence W_E scales as f^2 for $f \ll 1/t$ and as $1/f^2$ for $f \gg 1/t$. In this case, we expect the dominant contribution to the dephasing time to be from noise at frequencies $f \approx 1/\tau_{\phi,E}$.

The decay function $g(t)$ is calculated by ensemble averaging over the entire measurement time, yielding[4,29]

$$g(t) = \exp\left[-t^2(2\pi D_\Phi)^2 \int_{f_1}^{f_2} df\, S_\Phi(f) W(f,t)\right]. \quad (4)$$

Here, the symmetrized noise power is defined as $S_\Phi(f) \equiv (1/2)\int dt\{\langle\Phi(t)\Phi(0)\rangle + \langle\Phi(0)\Phi(t)\rangle\}e^{-2\pi i f t}$, which we replace with the observed spectrum: $S_\Phi(f) = A^2/[f/(1\text{ Hz})]^\alpha$; f_1 and f_2 are cutoff frequencies limiting the noise frequency bandwidth to which the qubit is sensitive. Independent of the particular pulse sequence, the infrared cutoff f_1 is set by the entire measurement time T taken to acquire sufficient statistics to determine the decay function $g(t)$, that is, $f_1 = 1/T$, where T may range from, say, 1 ms to 1000 s. What determines the ultraviolet cutoff f_2, however, is less clear. Recent experiments[30,31] indicate that flux noise can not only extend to very high frequencies (in one case in excess of 1 GHz) but also maintain its nonunity value of α out to f_2.

B. Dephasing times versus α

As is evident from Eq. (4), a nonunity value of α will affect the integral in a complicated way. Figure 3 shows computed dephasing times for both sequences versus α for $f_2 \to \infty$ and $f_1 = 10^{-3}$, 10^{-1}, 10^1, and 10^3 Hz. The effect of changing α is substantial: both $\tau_{\phi,R}$ and $\tau_{\phi,E}$ increase by an order of magnitude as α is varied from 0.6 to 0.9. By comparison, we find that an order of magnitude change in A for a given value of α also changes τ_ϕ by an order of magnitude. Figure 3 further shows that, because of its insensitivity to low-frequency noise, the echo sequence yields significantly longer dephasing times for all α. Finally, while $\tau_{\phi,E}$ is insensitive to changes in f_1 for $f_1 \ll 1/\tau_{\phi,E}$ (equivalently $T \gg \tau_{\phi,E}$), $\tau_{\phi,R}$ becomes increasingly sensitive as α increases.

C. Dephasing times versus cutoff frequencies

We now examine more quantitatively the sensitivity of τ_ϕ to changes in both f_1 and f_2 for various values of α. For

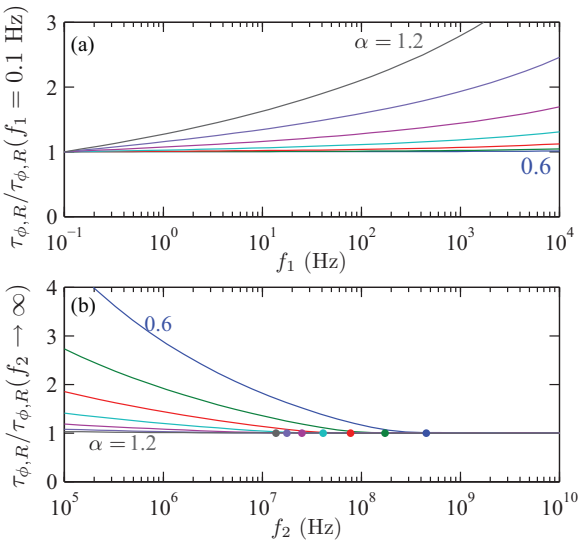

FIG. 4. (Color online) Normalized Ramsey dephasing times for $0.6 \leqslant \alpha \leqslant 1.2$ in steps of 0.1. (a) $\tau_{\phi,R}(f_1)/\tau_{\phi,R}(f_1 = 0.1\text{ Hz})$ versus f_1 for $f_2 \to \infty$ and (b) $\tau_{\phi,R}(f_2)/\tau_{\phi,R}(f_2 \to \infty)$ versus f_2. The dots in (b) are placed at $f_2 = 1/\tau_{\phi,R}(f_2 \to \infty)$, above which $\tau_{\phi,R}$ displays no dependence on f_2 (see text).

the Ramsey sequence with $f_2 \to \infty$, Fig. 4(a) shows $\tau_{\phi,R}$, normalized to $\tau_{\phi,R}(f_1 = 0.1\text{ Hz})$ versus f_1 for $0.6 \leqslant \alpha \leqslant 1.2$. We again see that the sensitivity of $\tau_{\phi,R}$ to f_1 increases with increasing α. Even so, for $\alpha = 1.2$, $\tau_{\phi,R}$ changes by a factor of only 4 when f_1 is varied from 0.1 to 10^4 Hz.

To explore the effect of f_2 on $\tau_{\phi,R}$, we fix $f_1 = 1$ Hz and vary f_2, plotting $\tau_{\phi,R}(f_2)/\tau_{\phi,R}(f_2 \to \infty)$ for $0.6 \leqslant \alpha \leqslant 1.2$ [Fig. 4(b)]. We see that the sensitivity of $\tau_{\phi,R}$ to f_2 increases for decreasing α. Furthermore, Fig. 4(b) shows that $\tau_{\phi,R}$ is insensitive to the particular value of f_2 for $f_2 \gg 1/\tau_{\phi,R}(f_2 \to \infty)$, simply because the Ramsey sequence is insensitive to noise for $f \gg 1/\tau_{\phi,R}$. However, as f_2 decreases through $1/\tau_{\phi,R}(f_2 \to \infty)$ a non-negligible amount of noise to which the qubit is sensitive is effectively eliminated, thereby reducing the total integrated noise and increasing $\tau_{\phi,R}(f_2)$. This effect is greater for small α, where S_Φ decreases with f more slowly and contributes to dephasing out to a higher frequency.

We perform a similar analysis of the sensitivity of $\tau_{\phi,E}$ to the value of f_2. In Fig. 5 we plot $\tau_{\phi,E}(f_2)/\tau_{\phi,E}(f_2 \to \infty)$ versus f_2 for $f_1 = 1$ Hz. As with the Ramsey sequence, we find that $\tau_{\phi,E}$ is insensitive to f_2 for $f_2 \gg 1/\tau_{\phi,E}(f_2 \to \infty)$. Indeed, since $\tau_{\phi,E}$ is dominated by noise at $f \approx 1/\tau_{\phi,E}$, this result is as we expect. Also in analogy with the Ramsey sequence, $\tau_{\phi,E}$ is more sensitive to f_2 for small α. Unlike the Ramsey sequence, however, where the dephasing is sensitive to frequencies over a large bandwidth (f_1 to $1/\tau_{\phi,R}$), the echo sequence is sensitive to noise only in a narrow bandwidth around $1/\tau_{\phi,E}$, making $\tau_{\phi,E}$ much more sensitive to changes in f_2 for $f_2 \approx 1/\tau_{\phi,E}$. Here, $\tau_{\phi,E}$ increases by an order of magnitude for a two-order-of-magnitude decrease in f_2.

D. The ratio $\tau_{\phi,E}/\tau_{\phi,R}$

Since the value D_ϕ can vary significantly between flux qubits, we consider the ratio $\tau_{\phi,E}/\tau_{\phi,R}$, which has the advantage of being rather insensitive to the precise values of

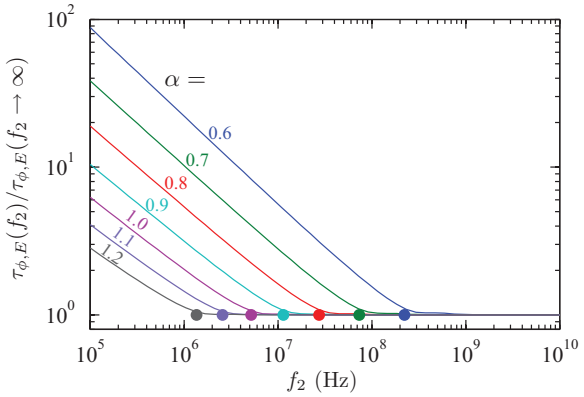

FIG. 5. (Color online) Computed values of $\tau_{\phi,E}(f_2)/\tau_{\phi,E}(f_2 \to \infty)$ vs. f_2. Lower cutoff frequency $f_1 = 1$ Hz and $0.6 \leqslant \alpha \leqslant 1.2$ in steps of 0.1. The colored dots are placed at $f_2 = 1/\tau_{\phi,E}(f_2 \to \infty)$, above which $\tau_{\phi,E}$ displays no dependence on f_2 (see text).

both A and D_ϕ. We compute these times using Eq. (4), which shows that the decay function $g(t)$ depends only on the product AD_ϕ. To explore the dependence of the ratio on α, we compute $\tau_{\phi,E}/\tau_{\phi,R}$ versus α for $f_2 \to \infty$ (equivalent to $f_2 \gg 1/\tau_\phi$) and $f_1 = 10^{-1}$, 10^1, and 10^3 Hz. Furthermore, for each value of f_1 we perform the calculation for $AD_\phi/(10^6\ \text{Hz}^{1/2}) = 0.2$, 1, and 5. The results are shown in Fig. 6.

First, we examine the dependence on α. As α increases, noise at frequencies much greater than 1 Hz falls quickly, so $\tau_{\phi,E}$ increases rapidly. Conversely, noise at low frequencies near 1 Hz changes little as α changes. The Ramsey dephasing time is sensitive to a large noise bandwidth where a significant contribution comes from frequencies near f_1. Therefore, as α increases we expect $\tau_{\phi,R}$ to increase less rapidly than $\tau_{\phi,E}$, explaining the increasing trend of $\tau_{\phi,E}/\tau_{\phi,R}$

For small, fixed values of α, changing the value of f_1 changes the ratio only slowly because both $\tau_{\phi,E}$ and $\tau_{\phi,R}$ are limited by noise at $f \gg f_1$. As the value of α increases, however, an increasing contribution to dephasing in the Ramsey sequence arises from lower frequencies $f \approx f_1$. Therefore, for large, fixed values of α, increasing f_1 has the effect of removing a significant noise contribution, thereby increasing $\tau_{\phi,R}$ and

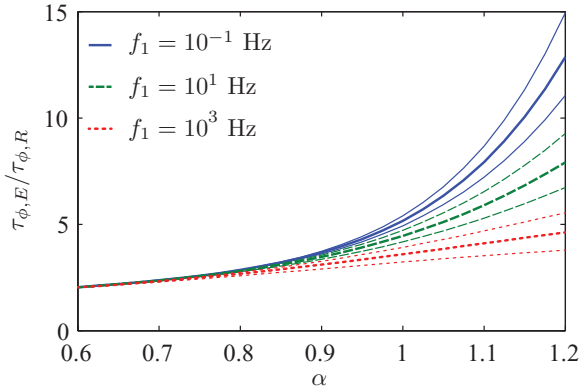

FIG. 6. (Color online) Ratio $\tau_{\phi,E}/\tau_{\phi,R}$ vs. α. Lower cutoff frequency $f_1 = 10^{-1}$, 10^1, and 10^3 Hz and $f_2 \to \infty$. The thin upper, heavy middle, and thin lower lines correspond to $AD_\phi/(10^6\ \text{Hz}^{1/2}) = 0.2$, 1, and 5, respectively.

decreasing the ratio $\tau_{\phi,E}/\tau_{\phi,R}$. We remark that since f_1 is an experimentally variable parameter, measuring $\tau_{\phi,E}/\tau_{\phi,R}$ for several different measurement times may shed light on the value of α.

Finally, we see that the $\tau_{\phi,E}/\tau_{\phi,R}$ is moderately sensitive to the product AD_ϕ only for $\alpha \gtrsim 1$. However, additional calculations show that, for $f_2 \lesssim 1/\tau_\phi$, the ratio becomes extremely sensitive to the particular value of AD_ϕ.

E. Dependence of decay function on α and ultraviolet cutoff frequency

The decay function is of particular interest experimentally, since it can be measured directly. In general, the decay function of T_1-limited processes is a simple exponential, that is, $g(t) = \exp(-t/T_1)$. However, the decay function of pure dephasing processes is more complicated and can be characterized as $g(t) \equiv \exp[-\chi(t)]$, where $\chi(t)$ can contain terms that are higher order in t.

Here, we examine the functional dependence of $\chi(t)$ for both pulse sequences. In each case, we find that $\chi(t) \propto t^\gamma$, where γ can take two values (γ_1 and γ_2) within a single sequence, separated by a characteristic time set by $1/f_2$: $\chi(t \ll 1/f_2) \propto t^{\gamma_1}$ and $\chi(t \gg 1/f_2) \propto t^{\gamma_2}$. For the Ramsey sequence, $\gamma_1 = 2$ and $\gamma_2 = 1 + \alpha$ for $\alpha \leqslant 1$ and $\gamma_2 = 2$ for $\alpha > 1$. For the echo sequence, $\gamma_1 = 4$ and $\gamma_2 = 1 + \alpha$. These results reveal two experimentally relevant insights. First, for $t \gg 1/f_2$, γ_2 depends on α. Thus, if $\tau_\phi \gg 1/f_2$, a careful fit of the experimentally observed decay envelope may shed light on the value of α. Second, the functional form of $g(t)$ can reveal information about f_2. For example, if one does not observe that $\chi(t) \propto t^4$ in an echo experiment, f_2 must be as high as $1/\tau_{\phi,E}$, establishing an important lower bound on the bandwidth of the flux noise.

Figure 7 emphasizes the above statements, showing $g(t)$ plotted for both sequences for $\alpha = 0.6$ and 1.2, and for f_2 both above and below $1/\tau_\phi(f_2 \to \infty)$, thereby showing both γ_1 and γ_2 dependence. In Figs. 7(a) and 7(b) we plot $g(t)$ for the Ramsey sequence with $\alpha = 0.6$ and 1.2. We note that

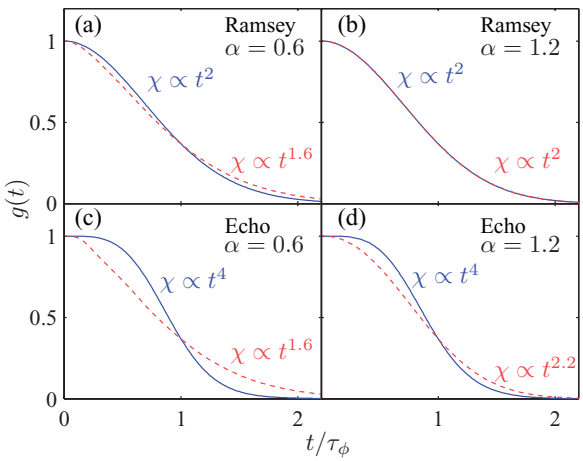

FIG. 7. (Color online) Computed decay function $g(t)$ versus t/τ_ϕ for (a) and (b) Ramsey sequences and (c) and (d) echo sequences with $\alpha = 0.6$ and 1.2. In the dashed red trace, $f_2 \gg 1/\tau_\phi(f_2 \to \infty)$; in the solid blue trace $f_2 \ll 1/\tau_\phi(f_2 \to \infty)$.

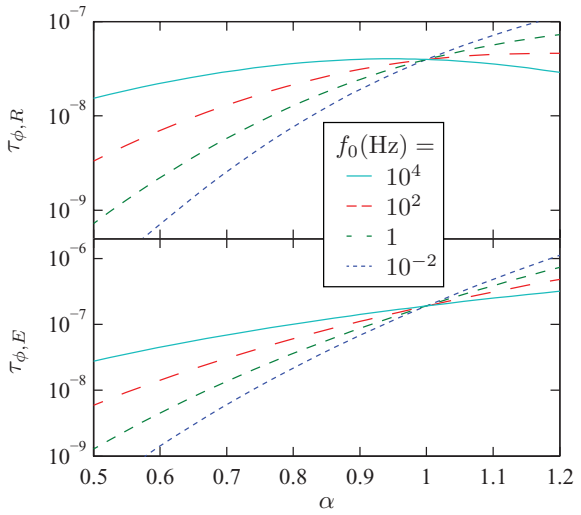

FIG. 8. (Color online) Computed dephasing times τ_ϕ vs. α for $f_1 = 1$ Hz and $f_2 \to \infty$. (a) Ramsey and (b) echo pulse sequences for fixed $S_\Phi(f_0)$, where the pivot frequency $f_0 = 10^{-2}$, 1, 10^2, and 10^4 Hz.

the difference between the functional dependencies of the two traces in Fig. 7(a) is slight and would be nearly impossible to measure experimentally. In Fig. 7(b) there is no functional difference since $\gamma_1 = \gamma_2$. Figures 7(c) and 7(d) show $g(t)$ for the echo sequence for $\alpha = 0.6$ and 1.2. The difference is more dramatic since $\gamma_1 = 4$ is so large. In this case, such a difference might be experimentally observable.

F. $S_\Phi(f)$ pivoting about $f_0 \neq 1$ Hz as α is varied

As mentioned previously, there is no *a priori* reason to hold $S_\Phi(1\text{ Hz})$ fixed as α is varied; the choice is based on the empirical observation that values of $S_\Phi(1\text{ Hz})$ are relatively uniform across a wide variety of devices and measured α. To explore the sensitivity of our calculations to this assumption, we calculated the dephasing times for both sequences versus α for fixed $S_\Phi(f_0)$, where $f_0 = 10^{-2}$, 1, 10^2, and 10^4 Hz. Conceptually, the spectra can be imagined as pivoting as α changes about a fixed spectral density $S_\Phi(f_0)$ at frequency f_0. In order to normalize the magnitude of each set of curves corresponding to a particular f_0, we choose as a convention that $S_\Phi(1\text{ Hz}) = A^2$ when $\alpha = 1$, regardless of the value of f_0, that is, $S_\Phi(f) = (A^2/f_0)(f/f_0)^{-\alpha}$. This convention is based loosely on empirical observation; it does not significantly change the dependence of τ_ϕ on α, but merely sets the absolute scale.

The results of these calculations, plotted in Fig. 8, show a dramatic effect, both qualitatively and quantitatively, on the dependence of $\tau_{\phi,R}$ and $\tau_{\phi,E}$ on α. For the Ramsey sequence [Fig. 8(a)], the general trend of increasing $\tau_{\phi,R}$ is significantly altered as f_0 increases and even becomes nonmonotonic for $f_0 = 10^4$ Hz. In addition, for small values of α, $\tau_{\phi,R}$ increases dramatically as f_0 increases. We note that, because of our normalization condition, the curves intersect at $\alpha = 1$. Calculations for the echo sequence are shown in Fig. 8(b), which shows a similar dependence of $\tau_{\phi,E}$ on f_0. For both sequences, the dependence of τ_ϕ on α is minimal for $f_0 = 10^4$ Hz, the highest computed f_0. This dependence is easily understood for the echo sequence, which is sensitive only to noise at $f \approx 1/\tau_{\phi,E}$. As f_0 approaches $1/\tau_{\phi,E}$, the effect of α eventually becomes negligible. In fact, if f_0 were to exceed $1/\tau_{\phi,E}$, the trend in α would actually reverse. The Ramsey sequence, however, is sensitive to a larger noise bandwidth and has a correspondingly more complicated dependence, exhibited by its nonmonotonic behavior for large values of f_0.

TABLE I. Computed $\tau_{\phi,R}$ and $\tau_{\phi,E}$ with $f_1 = 1$ Hz and $f_2 \to \infty$ for flux qubits with $I_q = 0.3$ μA. (Upper section) Values of A and α from Fig. 2; (middle section) A reduced by factor of 10, α unchanged; (lower section) A set equal to 1 $\mu\Phi_0\,\text{Hz}^{-1/2}$, α unchanged.

$A(\mu\Phi_0\,\text{Hz}^{-1/2})$	α	$\tau_{\phi,R}$ (ns)	$\tau_{\phi,E}$ (ns)
1.78	0.61	1.2	2.5
1.98	0.79	5.6	15.4
3.35	0.95	8.9	37.8
0.178	0.61	20.9	43.2
0.198	0.79	73.3	202.5
0.335	0.95	99.5	400.8
1.0	0.61	2.4	5.1
1.0	0.79	11.9	33.1
1.0	0.95	31.6	130.5

G. Tabulated dephasing times

Finally, we use our theoretical prediction of a strong dependence of the dephasing times on α to calculate $\tau_{\phi,R}$ and $\tau_{\phi,E}$ for the experimental values of A and α shown in Fig. 2. We assume $f_1 = 1$ Hz and $f_2 \to \infty$. The results are shown in the upper section of Table I. We see that, despite having the largest value of the flux noise magnitude A, the spectrum with the highest value of α, 0.95, yields the longest dephasing times. This result emphasizes a crucial point: simply lowering the flux noise magnitude A while keeping α constant may not be the most effective avenue to increasing τ_ϕ. The middle section of Table I shows the effect on $\tau_{\phi,R}$ and $\tau_{\phi,E}$ of a 10-fold reduction in A for fixed α. The factors by which $\tau_{\phi,R}$ and $\tau_{\phi,E}$ increase are comparable and decrease as α increases, from about 17 ($\alpha = 0.61$) to about 11 ($\alpha = 0.95$). The values of $\tau_{\phi,R}$ and $\tau_{\phi,E}$ for $A = 1\mu\Phi_0\,\text{Hz}^{-1/2}$ are shown in the lower section of Table I. As expected, $\tau_{\phi,R}$ and $\tau_{\phi,E}$ increase dramatically as α increases from 0.61 to 0.95.

IV. CONCLUDING REMARKS

In conclusion, we have presented data showing that, in general, flux noise scales as $1/f^\alpha$, where $0.6 \lesssim \alpha \lesssim 1.0$. Our subsequent calculations show that the predicted dephasing times $\tau_{\phi,R}$ and $\tau_{\phi,E}$ of a qubit are very sensitive to the value of α. As the value of α increases, both $\tau_{\phi,R}$ and $\tau_{\phi,E}$ increase dramatically—by an order of magnitude in some cases. Since experimentally inferred values of $S_\Phi(1\text{ Hz})$ from qubit measurements have generally assumed that $\alpha = 1$, a nonunity value of α can introduce a significant error into the inferred value of A. Furthermore, we have shown that while the lower cutoff frequency f_1 (set by the total measurement time) does not significantly affect τ_ϕ, the upper frequency cutoff

f_2 can significantly change τ_ϕ in a manner dependent on the value of α, particularly for the echo sequence. Moreover, we have shown that by examining the directly measurable ratio $\tau_{\phi,E}/\tau_{\phi,R}$ and the dephasing function $g(t)$, experimentalists may have a probe into the values of α and f_2. Finally, the frequency at which the flux noise spectra pivot can dramatically affect the sensitivity of τ_ϕ to α.

Most importantly, these results demonstrate that lowering the flux noise amplitude is not the only method of increasing qubit dephasing times. With a more detailed understanding of what sets α experimentally—for example, the geometry of the qubit washer—it may be possible to increase dephasing times substantially by raising the value of α. Finally, we note that with straightforward modification our formalism could be used to calculate dephasing times from critical current noise and charge noise for the case $\alpha \neq 1$.

ACKNOWLEDGMENTS

This research was funded by the CFN of the DFG and by the Office of the Director of National Intelligence (ODNI), Intelligence Advanced Research Projects Activity (IARPA), through the Army Research Office.

*Present address: Laboratoire de Physique Statistique de l'Ecole Normale Supérieure, associé au CNRS et aux Universités Denis Diderot et P.M. Curie, 24 rue Lhomond 75231 Paris Cedex 05, France.

[1] J. Clarke and F. K. Wilhelm, Nature **453**, 1031 (2008).
[2] Y. Nakamura, C. D. Chen, and J. Tsai, Phys. Rev. Lett. **79**, 2328 (1997).
[3] C. H. van der Waal, A. C. J. ter Haar, F. K. Wilhelm, R. N. Schouten, C. J. P. M. Harmans, T. P. Orlando, S. Lloyd, and J. E. Mooij, Science **290**, 773 (2000).
[4] J. M. Martinis, S. Nam, J. Aumentado, and C. Urbina, Phys. Rev. Lett. **89**, 117901 (2002).
[5] Y. Makhlin, G. Schön, and A. Shnirman, Rev. Mod. Phys. **73**, 357 (2001).
[6] R. H. Koch, J. Clarke, W. M. Goubau, J. M. Martinis, C. M. Pegrum, and D. J. Harlingen, J. Low Temp. Phys. **51**, 207 (1983).
[7] F. C. Wellstood, C. Urbina, and J. Clarke, Appl. Phys. Lett. **50**, 772 (1987).
[8] D. Drung, J. Beyer, J. Storm, M. Peters, and T. Schurig, IEEE Trans. Appl. Supercond. **21**, 340 (2011).
[9] S. Sendelbach, D. Hover, A. Kittel, M. Mück, J. M. Martinis, and R. McDermott, Phys. Rev. Lett. **100**, 227006 (2008).
[10] D. Sank, R. Barends, R. C. Bialczak, Y. Chen, J. Kelly, M. Lenander, E. Lucero, M. Mariantoni, M. Neeley, P. J. J. O'Malley *et al.*, arxiv:1111.2890.
[11] R. H. Koch, D. P. DiVincenzo, and J. Clarke, Phys. Rev. Lett. **98**, 267003 (2007).
[12] L. Faoro and L. B. Ioffe, Phys. Rev. Lett. **100**, 227005 (2008).
[13] S. K. Choi, D.-H. Lee, S. G. Louie, and J. Clarke, Phys. Rev. Lett. **103**, 197001 (2009).
[14] H. Bluhm, J. A. Bert, N. C. Koshnick, M. E. Huber, and K. A. Moler, Phys. Rev. Lett. **103**, 026805 (2009).
[15] F. Yoshihara, Y. Nakamura, and J. S. Tsai, Phys. Rev. B **81**, 132502 (2010).
[16] S. Gustavsson, J. Bylander, F. Yan, W. D. Oliver, F. Yoshihara, and Y. Nakamura, arXiv:1104.5212.
[17] S. Sendelbach, D. Hover, M. Mück, and R. Mc Dermott, Phys. Rev. Lett. **103**, 117001 (2009).
[18] Z. Chen and C. C. Yu, Phys. Rev. Lett. **104**, 247204 (2010).
[19] K. Kechedzhi, L. Faoro, and L. B. Ioffe, arXiv:1102.3445.
[20] J. Wu and C. Yu, arXiv:1111.2056.
[21] F. Yoshihara, K. Harrabi, A. O. Niskanen, Y. Nakamura, and J. S. Tsai, Phys. Rev. Lett. **97**, 167001 (2006).
[22] K. Kakuyanagi, T. Meno, S. Saito, H. Nakano, K. Semba, H. Takayanagi, F. Deppe, and A. Shnirman, Phys. Rev. Lett. **98**, 047004 (2007).
[23] T. Lanting, A. Berkley, B. Bumble, P. Bunyk, A. Fung, J. Johansson, A. Kaul, A. Kleinsasser, E. Ladizinsky, F. Maibaum *et al.*, Phys. Rev. B **79**, 060509(R) (2009).
[24] R. Bialczak, R. Mc Dermott, M. Ansmann, M. Hofheinz, N. Katz, E. Lucero, M. Neeley, A. O'connell, H. Wang, A. Cleland *et al.*, Phys. Rev. Lett. **99**, 187006 (2007).
[25] J. Sauvageau, C. Burroughs, P. Booi, M. Cromar, R. Benz, and J. Koch, IEEE Trans. Appl. Supercond. **5**, 2303 (1995).
[26] T. P. Orlando, J. E. Mooij, L. Tian, C. H. van der Wal, L. S. Levitov, S. Lloyd, and J. J. Mazo, Phys. Rev. B **60**, 15398 (1999).
[27] N. F. Ramsey, Phys. Rev. **78**, 695 (1950).
[28] E. L. Hahn, Phys. Rev. **80**, 580 (1950).
[29] G. Ithier, E. Collin, P. Joyez, P. J. Meeson, D. Vion, D. Esteve, F. Chiarello, A. Shnirman, Y. Makhlin, J. Schriefl *et al.*, Phys. Rev. B **72**, 134519 (2005).
[30] J. Bylander, S. Gustavsson, F. Yan, F. Yoshihara, K. Harrabi, G. Fitch, D. G. Cory, Y. Nakamura, J.-S. Tsai, and W. D. Oliver, Nat. Phys. **7**, 565 (2011).
[31] D. H. Slichter *et al.* (unpublished).